Quasilinear infiltration from an elliptical cavity

Kristopher L. Kuhlman [a] Arthur W. Warrick [b]

[a] *Department of Hydrology & Water Resources, University of Arizona, Tucson, Arizona 85721, USA*

[b] *Department of Soil, Water & Environmental Science, University of Arizona, Tucson, Arizona 85721, USA*

Abstract

We develop analytic solutions to the linearized steady-state Richards equation for head and total flowrate due to an elliptic cylinder cavity with a specified pressure head boundary condition. They are generalizations of the circular cylinder cavity solutions of Philip (1984). The circular and strip sources are limiting cases of the elliptical cylinder solution, derived for both horizontally- and vertically-aligned ellipses. We give approximate rational polynomial expressions for total flowrate from an elliptical cylinder over a range of sizes and shapes. The exact elliptical solution is in terms of Mathieu functions, which themselves are generalizations of and computed from trigonometric and Bessel functions. The required Mathieu functions are computed from a matrix eigenvector problem, a modern approach that is straightforward to implement using available linear algebra libraries. Although less efficient and potentially less accurate than the iterative continued fraction approach, the matrix approach is simpler to understand and implement and is valid over a wider parameter range.

Key words: quasilinear, Richards' equation, analytic solution, elliptic cylinder coordinates, Mathieu functions

1 Introduction

A solution for flow from a long elliptic cylinder cavity is given in two-dimensional elliptical coordinates for the quasilinear (Philip, 1968) form of the steady unsaturated flow equation (Richards, 1931) in a homogeneous porous medium.

* Corresponding author. Tel.: + 1 520 621 1380
Email address: kuhlman@hwr.arizona.edu (Kristopher L. Kuhlman).

The solution is an extension of one by Philip (1984) for flow from a circular cylinder cavity.

The approach taken here is to expand the linearized potential in the natural eigenfunctions that arise in elliptical coordinates. This technique has been utilized extensively in the physics literature (e.g., Stratton (1941, §6.12), Chu and Stratton (1941), Morse and Feshbach (1953, p.1407–1432), Moon and Spencer (1961a), Arscott (1964), and Kleinermann et al. (2002)), but the solution derived here for the current problem's boundary conditions is new.

Unsaturated porous media flow, specifically infiltration, is a very non-linear process that is often solved numerically with finite element codes such as HYDRUS-2D (e.g., Skaggs et al. (2004)). Analytic solutions to infiltration problems, restricted as they may be, often deliver more insightful results due to their simplicity. They give solutions with fewer potentially complicating auxiliary parameters. Pullan (1990) reviews the history of the quasilinear solution methodology and compares numerous approaches for solving the linearized Richards equation.

In the context of predicting furrow infiltration, Rawls et al. (1990) compared steady infiltration solutions for 1, 2, and 3 dimensions, using the 2D point source solution of Philip (1968) in the comparison. The solution derived here for an elliptical shape is more realistically furrow-shaped; ellipses have the capability of simulating the geometry associated with either wide or deep cavities and strips, rather than simple point approximations. Warrick et al. (2007) and Warrick and Lazarovitch (2007) discuss the impacts that dimensionality and "edge effects" have on infiltration from strips and parabolic-shaped furrows.

The elliptical solution derived here can represent the geometry of a strip or furrow explicitly, although without surface or water table boundary effects. It is a free-space solution, since it is valid at large distance. A dry far-field condition is assumed, resulting in no-flow far away from the ellipse. Including the effects of the land surface (potentially intersecting the ellipse) would require imposing a no-flow boundary condition. This homogeneous type II boundary condition would become an inhomogeneous type III boundary condition after applying the required non-linear transformations (Wooding, 1968). A solution for flow from an elliptical cavity that accounted for this boundary condition would most likely be approximate in nature (e.g., a linearized AEM or gridded numerical solution). An alternative approach would be to use the integral expression of Lomen and Warrick (1978, eq.5) (with $D = 0$, and no dependence on Y or T) to include the effects of a horizontal evaporative or no-flow boundary. Similarly, Philip (1989) and Warrick (2003, p.276) indicate how a water table condition can be accounted for with a free-space solution. Using the solution derived here in these integral relationships leads to integral expressions that cannot be evaluated in closed form for general values of the coordinates.

Bakker and Nieber (2004) applied the analytic element method to the quasi-linear flow equation for the problem of uniform vertical flow through ellipses of different material properties. Their approach is quite general, but to obtain a solution for multiple elements involves performing two nested iterations. A non-linear boundary-matching iteration is nested within an outer iteration that accounts for the effects elements have on one another. In the analysis presented here, no iterations are required to compute the solution, outside of those potentially needed to compute the required Mathieu functions (also needed for the AEM solution).

Mathieu functions are the special functions that arise as solutions to the Helmholtz equation in elliptic-cylinder coordinates (Morse and Feshbach (1953, p.562), Moon and Spencer (1961b), Arscott and Darai (1981), and Ben-Menahem and Singh (2000, p.53)). We use a modern matrix eigenvector approach (Stamnes and Spjelkavik, 1995; Chaos-Cador and Ley-Koo, 2002), allowing all the required functions and coefficients to be computed using any combination of widely available eigensolution (e.g., Matlab (MathWorks, 2007) or LAPACK (Golub and van Loan, 1996)) and Bessel function routines.

2 Governing equation

2.1 Quasilinear flow equation

The steady-state unsaturated porous media flow equation (Richards, 1931) is

$$\widehat{\nabla} \cdot \left(K(h) \widehat{\nabla} h \right) = \frac{\partial K}{\partial z}, \tag{1}$$

where $K(h)$ is hydraulic conductivity $[L/T]$, a non-linear function of pressure head, h $[L]$. Flow is driven by gradients in hydraulic head, $\Phi = h - z$, the sum of pressure and elevation heads (z positive down). Hats indicate dimensional differential operators. The Kirchhoff transformation (Klute, 1952) is used to linearize (1); it is

$$\Theta(h) = \int_{-\infty}^{h} K(u)\, \mathrm{d}u, \tag{2}$$

where u is a dummy variable and Θ is matric flux potential $[L^2/T]$. Applying (2) leads to

$$\widehat{\nabla}^2 \Theta = \frac{1}{K} \frac{\mathrm{d}K}{\mathrm{d}h} \frac{\partial \Theta}{\partial z}. \tag{3}$$

The Gardner (1958) exponential $K(h)$ distribution is used to simplify (3) further, by assuming the linearizing relationship $K(h) = K_0 e^{\alpha h}$, where $h < 0$ for unsaturated flow, α is the sorptive number $[1/L]$ (related to pore size) and

K_0 is K at saturation. With the Gardner distribution, (3) becomes

$$\widehat{\nabla}^2\Theta = \alpha\frac{\partial\Theta}{\partial z}, \tag{4}$$

the steady quasilinear form of Richards' equation. The quasilinear approximation was first extensively studied by Philip (1968); Pullan (1990) summarizes its benefits and limitations.

2.2 Elliptical geometry

A long elliptical pipe is represented as a surface of constant radius in two-dimensional elliptic-cylinder coordinates, where the variation along the length of the pipe is negligible. For a horizontal ellipse, the major axis is parallel to the land surface and the positive z-axis points down (see Figure 1). The elliptical angular coordinate starts at the positive x-axis and increases clockwise, $0 \leq \psi \leq 2\pi$. Cartesian coordinates (x, z) $[L]$ are defined in terms of the dimensionless elliptical coordinates (η, ψ) as

$$x = f\cosh(\eta)\cos(\psi), \qquad z = f\sinh(\eta)\sin(\psi), \tag{5}$$

where f is the semi-focal distance $[L]$; the cylindrical boundary is $\eta = \eta_0$. The eccentricity of the ellipse is a dimensionless quantity,

$$e = \sqrt{1 - \frac{b^2}{a^2}}, \tag{6}$$

equivalently given as $f = ea$, that ranges from 0 (circle) to 1 (line segment joining the foci). The pair (a, e) completely specifies the geometry of the problem; a is a measure of the size of the cavity, while e is related to its shape. The circumference of the ellipse, c $[L]$, cannot be evaluated exactly in closed form. It is defined by an elliptic integral, but can be approximated using one of several formulas. We use the simple YNOT expression (Maertens and Rousseau, 2000)

$$c \approx 4\sqrt[y]{a^y + b^y}, \tag{7}$$

where $y = \ln(2)/\ln\left(\frac{\pi}{2}\right)$ and the error in the approximation is at most 0.4%.

2.3 Non-dimensionalizing

Because of the problem's homogeneity, it can be made dimensionless with respect to the porous medium's sorptive number. Dimensionless lengths are defined

$$\frac{A}{a} = \frac{B}{b} = \frac{F}{f} = \frac{C}{c} = \frac{X}{x} = \frac{Z}{z} = \frac{\alpha}{2}, \tag{8}$$

where capital letters are dimensionless versions of lower-case variables. The dimensionless matric flux potential is $\vartheta = \Theta/\Theta(\eta_0)$. The boundary condition on the ellipse is specified pressure head, $h(\eta_0) = h_0$. For simplicity, the far-field boundary condition is no-flow,

$$h(\eta \to \infty) = -\infty, \qquad \Theta[h(\eta \to \infty)] = 0; \tag{9}$$

this corresponds to an assumption of dry conditions away from the cutout, i.e., the flow field is dominated by the moisture infiltrating from the ellipse.

The linearized flow equation (4) in dimensionless form, after the exponential substitution $\vartheta = He^Z$, becomes the Yukawa (Duffin, 1971) or modified Helmholtz equation,

$$\nabla^2 H = H; \tag{10}$$

(10) is subject to the boundary conditions

$$H(\eta_0, \psi) = e^{-F \sinh(\eta_0) \sin(\psi)} = e^{-B \sin(\psi)}, \tag{11}$$

$$H(\eta \to \infty) = He^{F \sinh(\eta) \sin(\psi)} \to 0, \tag{12}$$

in elliptical coordinates. Many solutions to (10) are available in the physics literature, though the combination of boundary condition (11) and elliptical geometry makes the solution derived here unique.

The dimensionless pressure ($\mathbf{\Psi}$) and hydraulic ($\mathbf{\Phi}$) heads are defined and related to ϑ by

$$\mathbf{\Psi} = \frac{h}{h - h_0} = \tfrac{1}{2}\ln(\vartheta), \qquad \mathbf{\Phi} = \frac{\Phi}{\Phi - h_0} = \tfrac{1}{2}\ln(\vartheta) - Z, \tag{13}$$

where we take $h_0 = 0$ for simplicity.

3 Solution via separation of variables

The dimensionless modified Helmholtz equation (10) in elliptical coordinates (Moon and Spencer, 1961b, p.17) is

$$\frac{2}{F^2\left[\cosh(2\eta) - \cos(2\psi)\right]}\left(\frac{\partial^2 H}{\partial \eta^2} + \frac{\partial^2 H}{\partial \psi^2}\right) = H. \tag{14}$$

We perform separation of variables by substituting $H(\eta, \psi) = R(\eta)Y(\psi)$, dividing by H, separating terms dependent on η from those dependent on ψ, and setting both quantities equal to the separation constant, λ; this results in

$$\frac{\mathrm{d}^2 R}{\mathrm{d}\eta^2} = R\left(2q\cosh(2\eta) + \lambda\right), \tag{15}$$

$$\frac{\mathrm{d}^2 Y}{\mathrm{d}\psi^2} = -Y\left(2q\cos(2\psi) + \lambda\right). \tag{16}$$

These are the radial (15) and angular (16) modified Mathieu equations (McLachlan, 1947). Here, λ is an eigenvalue chosen to make the angular solution, $Y(\psi)$, periodic for the specified value of the Mathieu parameter, $q = -F^2/4$. The solutions to equations (15) and (16) are radial and angular modified Mathieu functions; see Alhargan (2000), Gutiérrez Vega et al. (2003), or Bakker and Nieber (2004) for characteristic functional plots. The periodic solution to (16) and the corresponding free-space solution to (15) is

$$Y(\psi) = a_0 \mathrm{ce}_0(\psi; -q) + \sum_{n=1}^{\infty} a_n \mathrm{ce}_n(\psi; -q) + b_n \mathrm{se}_n(\psi; -q), \tag{17}$$

$$R(\eta) = c_0 \mathrm{Ke}_0(\eta; -q) + \sum_{n=1}^{\infty} c_n \mathrm{Ke}_n(\eta; -q) + d_n \mathrm{Ko}_n(\eta; -q), \tag{18}$$

where a_n, b_n, c_n, and d_n are coefficients to determine and $\mathrm{ce}_n(\psi; -q)$ and $\mathrm{se}_n(\psi; -q)$ are the even and odd, n^{th}-order, first-kind angular Mathieu functions of argument ψ and parameter $-q$. These functions degenerate to trigonometric functions as $q \to 0$ (see Appendix A for definitions). Similarly, $\mathrm{Ke}_n(\eta; -q)$ and $\mathrm{Ko}_n(\eta; -q)$ are the even and odd, n^{th}-order, second-kind radial Mathieu functions of argument η and parameter $-q$. Radial Mathieu functions are analogous to modified Bessel functions, degenerating to them as $q \to 0$.

The product of solutions to the Mathieu equations is a solution to (14),

$$H(\eta \geq \eta_0, \psi) = \sum_{n=0}^{\infty} \beta_n \frac{\mathrm{Ke}_n(\eta; -q)}{\mathrm{Ke}_n(\eta_0; -q)} \mathrm{ce}_n(\psi; -q) + \sum_{n=1}^{\infty} \gamma_n \frac{\mathrm{Ko}_n(\eta; -q)}{\mathrm{Ko}_n(\eta_0; -q)} \mathrm{se}_n(\psi; -q) \tag{19}$$

where β_n and γ_n are coefficients to determine and the radial Mathieu functions are normalized by their value on the boundary of the ellipse. Cross-products involving both odd and even functions are not considered because theses solutions correspond to different eigenvalues, which may only be combined via summation. At $\eta = \eta_0$, (19) simplifies to

$$H_0(\eta_0, \psi) = \beta_0 \mathrm{ce}_0(\psi; -q) + \sum_{n=1}^{\infty} \beta_n \mathrm{ce}_n(\psi; -q) + \gamma_n \mathrm{se}_n(\psi; -q). \tag{20}$$

3.1 Determination of coefficients

The orthogonality of the angular Mathieu functions is derived from the orthogonality of their sine and cosine components (McLachlan, 1947, §2.19);

$\int_0^{2\pi} \mathrm{ce}_n(\psi;q)\mathrm{se}_m(\psi;q)\ \mathrm{d}\psi = 0$ for any m, n, while

$$\int_0^{2\pi} \mathrm{se}_n(\psi;q)\mathrm{se}_m(\psi;q)\ \mathrm{d}\psi = \int_0^{2\pi} \mathrm{ce}_n(\psi;q)\mathrm{ce}_m(\psi;q)\ \mathrm{d}\psi = \pi\delta_{nm} \tag{21}$$

where δ_{nm} is the Kronecker delta and the two Mathieu functions share the same q. Multiplying (20) by each angular Mathieu function and integrating over the domain, integral expressions for the coefficients are

$$\beta_n = \frac{1}{\pi}\int_0^{2\pi} H_0(\eta_0,\psi)\mathrm{ce}_n(\psi;-q)\ \mathrm{d}\psi, \tag{22}$$

$$\gamma_n = \frac{1}{\pi}\int_0^{2\pi} H_0(\eta_0,\psi)\mathrm{se}_n(\psi;-q)\ \mathrm{d}\psi. \tag{23}$$

(22) is expanded using (11), (A-1), and (A-2) resulting in

$$\beta_{2n} = \frac{(-1)^n}{\pi}\sum_{r=0}^{\infty}(-1)^r \mathbf{A}_{2r}^{(2n)} \int_0^{2\pi} e^{-B\sin(\psi)}\cos(2r\psi)\ \mathrm{d}\psi, \tag{24}$$

$$\beta_{2n+1} = \frac{(-1)^n}{\pi}\sum_{r=0}^{\infty}(-1)^r \mathbf{B}_{2r+1}^{(2n+1)} \int_0^{2\pi} e^{-B\sin(\psi)}\cos\left[(2r+1)\psi\right]\ \mathrm{d}\psi. \tag{25}$$

where $\mathbf{A}$ and $\mathbf{B}$ are matrices of Mathieu coefficients (see Appendix B). Using an integral definition for the modified Bessel function of the first kind (Watson, 1944, §6.22), (24) simplifies to

$$\beta_{2n} = 2(-1)^n \sum_{r=0}^{\infty} \mathbf{A}_{2r}^{(2n)} \mathrm{I}_{2r}(B), \tag{26}$$

while (25) is zero for all integer r. This infinite sum of Bessel functions is equivalent to one of several definitions of a first-kind even radial Mathieu functions (A-8); this further simplifies the coefficient expression to

$$\beta_{2n} = 2p_{2n}\mathrm{Ie}_{2n}(\eta_0;-q), \tag{27}$$

where $p_{2n} = \mathbf{A}_0^{(2n)}/\mathrm{ce}_{2n}\left(\frac{\pi}{2};q\right)$. Similarly, γ_n are found to be

$$\gamma_{2n+1} = \frac{(-1)^n}{\pi}\sum_{r=0}^{\infty}(-1)^r \mathbf{A}_{2r+1}^{(2n+1)} \int_0^{2\pi} e^{-B\sin(\psi)}\sin\left[(2r+1)\psi\right]\ \mathrm{d}\psi \tag{28}$$

$$= 2(-1)^{n+1}\sum_{r=0}^{\infty} \mathbf{A}_{2r+1}^{(2n+1)} \mathrm{I}_{2r+1}(B), \tag{29}$$

$$= 2p_{2n+1}\mathrm{Io}_{2n+1}(\eta_0;-q) \tag{30}$$

where the integral involving se_{2n+2} is zero for all integer r, and $p_{2n+1} = \sqrt{q}\mathbf{A}_1^{(2n+1)}/\mathrm{ce}'_{2n+1}\left(\frac{\pi}{2};q\right)$, the prime indicating differentiation with respect to the argument.

Using (27) and (30), the solution for H from a horizontal ellipse is

$$H(\eta \geq \eta_0, \psi) \cong 2 \sum_{n=0}^{N-1} p_{2n} \mathrm{Ie}_{2n}(\eta_0; -q) \mathrm{ce}_{2n}(\psi; -q) \frac{\mathrm{Ke}_{2n}(\eta; -q)}{\mathrm{Ke}_{2n}(\eta_0; -q)} + p_{2n+1} \mathrm{Io}_{2n+1}(\eta_0; -q) \mathrm{se}_{2n+1}(\psi; -q) \frac{\mathrm{Ko}_{2n+1}(\eta; -q)}{\mathrm{Ko}_{2n+1}(\eta_0; -q)}. \quad (31)$$

The approximation comes from truncating the infinite sum at $2N-1$ terms. Eigenfunction expansions such as (31) share the favorable convergence properties of Fourier series (Morse and Feshbach (1953, p.743), Arscott (1964, §3.9.1)). Appendix B has some heuristic discussion on the level of approximation needed for most problems.

3.2 Limiting cases

3.2.1 Circular

As the ellipse becomes a circle, $[A, B] \rightarrow R_0$, the dimensionless circular radius. In the limit $q \rightarrow 0$, the eigenvector matrices, $\mathbf{A}_{2r}^{(2n)}$ and $\mathbf{A}_{2r+1}^{(2n+1)}$, become diagonal (see Appendix B); each angular Mathieu function is composed of a single harmonic ($n = r$). Therefore, the sum of coefficients in r reduce to a single term, $\mathrm{I}_{2n}(B)$.

The circular cylinder solution of Philip (1984) is derived for the coordinate system in Figure 1, resulting in a circular solution that corresponds to (31) as $e \rightarrow 0$,

$$H(R \geq R_0, \phi) \cong \frac{\mathrm{K}_0(R)}{\mathrm{K}_0(R_0)} \mathrm{I}_0(R_0) + 2 \sum_{n=1}^{N-1} (-1)^n \frac{\mathrm{K}_{2n}(R)}{\mathrm{K}_{2n}(R_0)} \mathrm{I}_{2n}(R_0) \cos(2n\phi) - 2 \sum_{m=0}^{N-1} (-1)^m \frac{\mathrm{K}_{2m+1}(R)}{\mathrm{K}_{2m+1}(R_0)} \mathrm{I}_{2m+1}(R_0) \sin\left[(2m+1)\phi\right], \quad (32)$$

where K_n is the second-kind modified Bessel function, $R = r\alpha/2$ is the dimensionless radius, and ϕ is the angle (following the convention in Figure 1). The integrals involving odd cosine orders and even sine orders are zero for all integer n.

Numerically, (31) is ill-behaved as $e \rightarrow 0$. The Mathieu functions do asymptotically become Bessel functions, but for $e \leq 0.01$ the solution is better approximated with (32).

3.2.2 Strip

In the other limiting case, as the elliptical cylinder degenerates to a strip ($e = 1$ and $B = 0$), the $\mathrm{I}_r(B)$ coefficients all become zero except $\mathrm{I}_0(0) = 1$, leaving

$$H(\eta \geq 0, \psi) \cong 2 \sum_{n=0}^{N-1} (-1)^n \mathbf{A}_0^{(2n)} \mathrm{ce}_{2n}(\psi; -q) \frac{\mathrm{Ke}_{2n}(\eta; -q)}{\mathrm{Ke}_{2n}(0; -q)}, \tag{33}$$

which is the same form given by Tranter (1951) and used by Kucûk and Brigham (1979) for the case of constant specified potential along an ellipse (not restricted to $\eta_0 = 0$ in their cases). When $B = 0$, the boundary condition on the ellipse (11) becomes constant; there is no z-variation across the strip. Numerically, (33) is well behaved; the radial Mathieu functions can be evaluated at $\eta = 0$ without problems.

3.3 Modification for vertically oriented ellipse

Since the modified Helmholtz equation (10) is symmetric with respect to x and z, the boundary conditions and back-transformation functions can be changed, to give the solution for a vertically-oriented ellipse. The domain is rotated clockwise by $\pi/2$ compared with Figure 1. The boundary condition is

$$\tilde{\vartheta}(\eta_0, \tilde{\psi}) = 1, \qquad \tilde{H}_0(\eta_0, \tilde{\psi}) = e^{-A\cos(\tilde{\psi})}, \tag{34}$$

where a tilde indicates the variable is related to the vertically-oriented ellipse ($\tilde{X}$ points down); the far-field boundary condition remains unchanged. (34) leads to modified expressions for the coefficients

$$\begin{aligned}
\tilde{\beta}_{2n} &= \frac{(-1)^n}{\pi} \sum_{r=0}^{\infty} (-1)^r \mathbf{A}_{2r}^{(2n)} \int_0^{2\pi} e^{-A\cos(\tilde{\psi})} \cos(2r\tilde{\psi}) \, \mathrm{d}\tilde{\psi} \\
&= 2(-1)^n \sum_{r=0}^{\infty} (-1)^r \mathbf{A}_{2r}^{(2n)} \mathrm{I}_{2r}(A), \qquad (35) \\
&= 2 s_{2n} \mathrm{Ie}_{2n}(\eta_0; -q), \\
\tilde{\beta}_{2n+1} &= \frac{(-1)^n}{\pi} \sum_{r=0}^{\infty} (-1)^r \mathbf{B}_{2r+1}^{(2n+1)} \int_0^{2\pi} e^{-A\cos(\tilde{\psi})} \cos\left[(2r+1)\tilde{\psi}\right] \, \mathrm{d}\tilde{\psi} \\
&= 2(-1)^{n+1} \sum_{r=0}^{\infty} (-1)^r \mathbf{B}_{2r+1}^{(2n+1)} \mathrm{I}_{2r+1}(A), \qquad (36) \\
&= -2 s_{2n+1} \mathrm{Ie}_{2n+1}(\eta_0; -q)
\end{aligned}$$

where now the integrals involving se_n are zero for integer r, $s_{2n} = \mathbf{A}_0^{(2n)}/\mathrm{ce}_{2n}(0;q)$, and $s_{2n+1} = \sqrt{q}\mathbf{B}_1^{(2n+1)}/\mathrm{se}'_{2n+1}(0;q)$. The solution for $\tilde{H}$, analogous to (31), is

$$\tilde{H}(\tilde{\eta} \geq \eta_0, \tilde{\psi}) \cong 2\sum_{n=0}^{N-1}(-1)^n s_n \mathrm{Ie}_n(\eta_0;-q)\mathrm{ce}_n(\tilde{\psi};-q)\frac{\mathrm{Ke}_n(\tilde{\eta};-q)}{\mathrm{Ke}_n(\eta_0;-q)}, \qquad (37)$$

which is very similar in form to equation 27 of Philip (1984).

This solution is back-transformed to dimensionless Cartesian coordinates using the definitions

$$\tilde{\vartheta} = \tilde{H}e^{\tilde{X}}, \qquad \tilde{X} = F\cosh(\tilde{\eta})\cos(\tilde{\psi}), \qquad \tilde{Z} = F\sinh(\tilde{\eta})\sin(\tilde{\psi}). \qquad (38)$$

The dimensionless potentials are

$$\tilde{\mathbf{\Psi}} = \frac{\tilde{h}}{\tilde{h}-h_0} = \frac{1}{2}\ln(\tilde{\vartheta}), \qquad \tilde{\mathbf{\Phi}} = \frac{\tilde{\Phi}}{\tilde{\Phi}-h_0} = \frac{1}{2}\ln(\tilde{\vartheta}) - \tilde{X}. \qquad (39)$$

The vertically-oriented solution (37) does not simplify in the limiting case $\eta_0 = 0$, due to its orientation; the source always has a boundary condition that varies with $\tilde{X}$.

4 Darcy flux along elliptical circumference

To determine the total flowrate, $\widehat{Q}$ $[L^3/T]$, and the average flux, $\overline{v}$ $[L/T]$, across the elliptical surface, the flux normal to the boundary of the ellipse is found, beginning with the dimensional form of Darcy's law,

$$\mathbf{v} = -K(h)\widehat{\nabla}\Phi, \qquad (40)$$

where $\mathbf{v}$ is the Darcy flux $[L/T]$. Expressing the gradient operator in elliptical coordinates (Moon and Spencer, 1961b) makes (40)

$$\mathbf{v} = \frac{-K(h)}{f\sqrt{\frac{1}{2}(\cosh(2\eta)-\cos(2\psi))}}\left(\frac{\partial\Phi}{\partial\eta}\mathbf{e}_\eta + \frac{\partial\Phi}{\partial\psi}\mathbf{e}_\psi\right), \qquad (41)$$

where $\mathbf{e}$ is a unit vector. For the horizontal ellipse, substituting $\Phi = h - f\sinh(\eta)\sin(\psi)$, using the notation $\xi(\eta,\psi) = \sqrt{\frac{1}{2}(\cosh(2\eta)-\cos(2\psi))}$, and taking the dot product with $\mathbf{e}_\eta$ gives

$$\mathbf{v}\cdot\mathbf{e}_\eta = \frac{K(h)}{f\xi(\eta,\psi)}\left[f\cosh(\eta)\sin(\psi) - \frac{\partial h}{\partial\eta}\right], \qquad (42)$$

for the radial (η) component of the flux. Evaluating (42) at $\eta = \eta_0$, applying the Kirchhoff transformation (2), using the Gardner exponential model, and non-dimensionalizing the flux leads to

$$V_0 = \frac{1}{F\xi(\eta_0,\psi)}\left\{2\sin(\psi) - \left[\frac{\partial\vartheta}{\partial\eta}\right]_{\eta_0}\right\}, \tag{43}$$

where $V_0 = 2\mathbf{v}(\eta_0)\cdot\mathbf{e}_\eta/(\Theta_0\alpha)$ and the subscript zero indicating the fluxes are evaluated on the boundary of the ellipse. The derivative in (43) can be expanded using the product rule as

$$\left[\frac{\partial\vartheta}{\partial\eta}\right]_{\eta_0} = e^{B\sin(\psi)}\left\{\left[\frac{\partial H}{\partial\eta}\right]_{\eta_0} + A\sin(\psi)H(\eta_0)\right\}, \tag{44}$$

where H and its radial derivative are computed from (31).

4.1 Average normal flux

Multiplying by $F\xi(\eta_0,\psi)$, the integral of (43) over $0 \le \psi \le 2\pi$ represents the weighted average dimensionless normal flux across the boundary of the ellipse, $\overline{V}_0$. This flux integral is found using the relationships from (24) and (29), along with the following integral relations

$$\begin{aligned}\int_0^{2\pi} e^{B\sin(\psi)}\sin(\psi)\mathrm{ce}_{2n}(\psi;-q)\,\mathrm{d}\psi &= 2\pi(-1)^n\sum_{r=0}^{\infty}\mathbf{A}_{2r}^{(2n)}\mathrm{I}'_{2r}(B),\\ &= 2\pi p_{2n}\mathrm{Ie}'_{2n}(\eta_0;-q),\end{aligned} \tag{45}$$

$$\begin{aligned}\int_0^{2\pi} e^{B\sin(\psi)}\sin(\psi)\mathrm{se}_{2n+1}(\psi;-q)\,\mathrm{d}\psi &= 2\pi(-1)^n\sum_{r=0}^{\infty}\mathbf{A}_{2r+1}^{(2n+1)}\mathrm{I}'_{2r+1}(B),\\ &= 2\pi p_{2n+1}\mathrm{Io}'_{2n+1}(\eta_0;-q),\end{aligned} \tag{46}$$

which can be found through trigonometric product identities, Bessel function derivative recurrence relationships, and definitions of the first-kind radial Mathieu functions (see Appendix A). Combining these, the expression for the average normal flux at the boundary of the ellipse is

$$\begin{aligned}\overline{V}_0 \cong -4\pi\sum_{n=0}^{N-1}&\left[p_{2n}\mathrm{Ie}_{2n}(\eta_0;-q)\right]^2\frac{\mathrm{Ke}'_{2n}(\eta_0;-q)}{\mathrm{Ke}_{2n}(\eta_0;-q)}\\ &+\left[p_{2n+1}\mathrm{Io}_{2n+1}(\eta_0;-q)\right]^2\frac{\mathrm{Ko}'_{2n+1}(\eta_0;-q)}{\mathrm{Ko}_{2n+1}(\eta_0;-q)}\\ &-A\mathrm{Ie}_{2n}(\eta_0;-q)\mathrm{Ie}'_{2n}(z;-q)\\ &-Ap_{2n+1}^2\mathrm{Io}_{2n+1}(\eta_0;-q)\mathrm{Io}'_{2n+1}(z;-q).\end{aligned} \tag{47}$$

The total flowrate is $Q = \overline{V}_0 C$, where C is the dimensionless elliptical circumference, given by (7) and (8).

When $B = 0$ and $\eta_0 = 0$, the average flux due to the strip source (47) simplifies to

$$\overline{V}_0(\eta_0 = 0) \cong -4\pi \sum_{n=0}^{N-1} \left[\mathbf{A}_0^{(2n)}\right]^2 \frac{\mathrm{Ke}'_{2n}(0; -q)}{\mathrm{Ke}_{2n}(0; -q)}. \tag{48}$$

4.2 Normal flux for vertical ellipse

Beginning again with (41), but instead substituting $\tilde{\Phi} = \tilde{h} - f\cosh(\tilde{\eta})\cos(\tilde{\psi})$, the dimensionless flux normal to the boundary of the vertical ellipse, analogous to (43), is

$$\tilde{V}_0 = \frac{1}{F\xi(\eta_0, \tilde{\psi})} \left\{ 2\cos(\tilde{\psi}) - \left[\frac{\partial \tilde{\vartheta}}{\partial \tilde{\eta}}\right]_{\eta_0} \right\}, \tag{49}$$

where the derivative in (49) is

$$\left[\frac{\partial \tilde{\vartheta}}{\partial \tilde{\eta}}\right]_{\eta_0} = e^{A\cos(\tilde{\psi})} \left\{ \left[\frac{\partial \tilde{H}}{\partial \tilde{\eta}}\right]_{\eta_0} + B\cos(\tilde{\psi})\tilde{H}(\eta_0) \right\}. \tag{50}$$

The average flux on the vertically-oriented ellipse is

$$\begin{aligned} \widetilde{\overline{V}}_0 \cong -4\pi \sum_{n=0}^{N-1} & \left[s_n \mathrm{Ie}_n(\eta_0; -q)\right]^2 \frac{\mathrm{Ke}'_n(\eta_0; -q)}{\mathrm{Ke}_n(\eta_0; -q)} \\ & - B s_n^2 \mathrm{Ie}_n(\eta_0; -q)\mathrm{Ie}'_n(w; -q), \end{aligned} \tag{51}$$

with the simplification for a strip source,

$$\widetilde{\overline{V}}_0(\eta_0 = 0) \cong -4\pi \sum_{n=0}^{N} \left[s_n \mathrm{Ie}_n(\eta_0; -q)\right]^2 \frac{\mathrm{Ke}'_n(0; -q)}{\mathrm{Ke}_n(0; -q)}. \tag{52}$$

5 Results and Comparisons

Contour plots of dimensionless hydraulic ($\mathbf{\Phi}$) and pressure ($\mathbf{\Psi}$) heads for the three cases of horizontal elliptical-shaped sources are given in Figure 2. The different source shapes are controlled by eccentricity; we illustrate $e = 0.9$ (ellipse-shaped), $e = 1$ (line segment), and $e = 0.01$ (nearly circular). The difference between the circular and elliptical cases when $e = 0.01$ and $A = R = 1.0$ is less than $1.5 \times 10^{-5}\mathbf{\Psi}$.

For the horizontal strip source (Figure 2), the specified h boundary condition degenerates to the constant boundary condition used by Tranter (1951) and Kucûk and Brigham (1979). For both the elliptical- and circular-shaped cavities, the variation in $\mathbf{\Phi}$ along the source boundary can be seen in the contour plots.

Figure 3 shows characteristic contours of $\tilde{\mathbf{\Phi}}$ and $\tilde{\mathbf{\Psi}}$ for the vertical elliptical and slit cases. Unlike the horizontal ellipse, the solution for the degenerate slit case (the line segment $-1 \leq \tilde{X} \leq 1$) does not simplify the boundary condition.

For plotting contour maps, such as those in Figures 2 and 3, a great deal of effort can be saved if the solution is computed on a "separated" elliptical mesh (Orszag, 1986). The angular Mathieu functions are computed for a vector of ψ and the radial Mathieu functions are computed for a vector of η, then they are combined in an outer-product sense. Many plotting programs can accommodate a non-Cartesian mesh, facilitating the use of this strategy.

The dimensionless flowrate, $Q = C\overline{V}_0$, is plotted on semi-log and log-log scales in Figure 4 for ranges of dimensionless semi-width, A, and eccentricity, e. For a given size, there is more water flowing from the circular cavity due to the greater surface area normal to flow. A horizontal ellipse (solid lines) deviates less from the circular solution (highest dash-dot line) than an equivalent vertical ellipse (dashed lines). This can be seen by comparing the location of the -0.25 $\mathbf{\Psi}$ contour in Figures 2 and 3; the vertical strip is smallest, while the circular cutout is largest. For ellipses where $e \leq 0.5$ the difference between the circular and elliptical solutions is minor.

To facilitate the use of this solution for computing steady flowrate from an strip, circle or furrow, second-degree rational polynomials were fitted to the curves in Figure 4 using least-squares. The polynomial coefficients are given in Table 1. The polynomial regression is performed in log-log space, where the curves take the form

$$\log_{10}\left[Q(A)\right] = \frac{c_0 + c_1 \log_{10}(A) + c_2 \left[\log_{10}(A)\right]^2}{1 + c_3 \log_{10}(A)}, \tag{53}$$

and the error in approximation is $\leq 1\%$ over $0.01 \leq A \leq 2$ (with slightly more error for large A in the vertical ellipse case).

The distribution of V_0 along the boundary of the ellipse, as a function of ψ, for different values of A, is given in Figure 5. For the larger cavity, the variation of flux along the circumference of the cavity is greater, due to the fact that the boundary condition strength is a function of the vertical coordinate.

6 Summary

We derived a two-dimensional solution in elliptic-cylinder coordinates for Richards' equation, illustrating its degeneration to the strip and circular cases. Infinite series expressions for the flowrate and flux from the elliptical cutout were also derived. The solutions are in terms of the eigenfunctions for elliptical coordinates, which themselves can be computed from infinite series of the eigenfunctions for polar coordinates.

Although the solutions developed herein are for free space, they represents strip and furrow geometries more realistically than the widely used point (Philip, 1968) or circular (Philip, 1984) solutions. To incorporate boundary conditions on horizontal surfaces, approximate boundary-matching techniques must be used (e.g., those used by Bakker and Nieber (2004)). The general solution (19) is in the form of an AEM solution, but the final forms (31 or 37) only have two free parameters beyond the geometry (α and h_0); flexible AEM elements commonly have many more. Analytic solutions usually have fewer free parameters than elements in AEM do, but this is what makes them simpler to use.

A short Matlab script which computes the required Mathieu functions and evaluates the dimensionless potentials and fluxes is available from the corresponding author upon request.

7 Acknowledgments

We would like to thank three anonymous reviewers for their insightful comments that improved the paper, making it more concise. The first author was supported in part by the USGS National Institutes for Water Resources Grant Program (award 200AZ68G) and by the C.W. & Modene Neely fellowship through the National Water Research Institute.

Appendix A

The modified angular Mathieu functions are defined as infinite series of trigonometric functions (see McLachlan (1947, §2.18)),

$$\mathrm{ce}_{2n}(\psi;-q) = (-1)^n \sum_{r=0}^{\infty}(-1)^r \mathbf{A}_{2r}^{(2n)} \cos[2r\psi], \tag{A-1}$$

$$\mathrm{ce}_{2n+1}(\psi;-q) = (-1)^n \sum_{r=0}^{\infty}(-1)^r \mathbf{B}_{2r+1}^{(2n+1)} \cos[(2r+1)\psi], \tag{A-2}$$

$$\mathrm{se}_{2n+1}(\psi;-q) = (-1)^n \sum_{r=0}^{\infty}(-1)^r \mathbf{A}_{2r+1}^{(2n+1)} \sin[(2r+1)\psi], \tag{A-3}$$

$$\mathrm{se}_{2n+2}(\psi;-q) = (-1)^n \sum_{r=0}^{\infty}(-1)^r \mathbf{B}_{2r+2}^{(2n+2)} \sin[(2r+2)\psi], \tag{A-4}$$

where $\mathbf{A}_r^{(n)}$ and $\mathbf{B}_r^{(n)}$ are matrices of the Mathieu coefficients (eigenvectors for each eigenvalue λ_n), they are the generalized Fourier series coefficients representing the Mathieu functions; see Appendix B.

The radial modified Mathieu functions of the second kind are used as solutions to the radial Mathieu equation (15) and are only evaluated in ratios of functions of the same kind and order, allowing them to be simplified from their definitions in terms of Bessel function product series (McLachlan, 1947, §13.30),

$$\mathrm{Ke}_{2n}(\eta;-q) = D_n \sum_{r=0}^{\infty} \mathbf{A}_{2r}^{(2n)} \mathrm{I}_r(v_1)\mathrm{K}_r(v_2), \tag{A-5}$$

$$\mathrm{Ke}_{2n+1}(\eta;-q) = D_n \sum_{r=0}^{\infty} \mathbf{B}_{2r+1}^{(2n+1)} \left[\mathrm{I}_r(v_1)\mathrm{K}_{r+1}(v_2) - \mathrm{I}_{r+1}(v_1)\mathrm{K}_r(v_2)\right], \tag{A-6}$$

$$\mathrm{Ko}_{2n+1}(\eta;-q) = D_n \sum_{r=0}^{\infty} \mathbf{A}_{2r+1}^{(2n+1)} \left[\mathrm{I}_r(v_1)\mathrm{K}_{r+1}(v_2) + \mathrm{I}_{r+1}(v_1)\mathrm{K}_r(v_2)\right], \tag{A-7}$$

where D_n is a normalization constant (not all the same) that is only a function of the order, $v_1 = \sqrt{q}e^{-\eta}$, $v_2 = \sqrt{q}e^{\eta}$, and the eigenvectors $\mathbf{A}_r^{(n)}$ and $\mathbf{B}_r^{(n)}$ are the same used in the angular Mathieu function definitions. The normalization constants can be found in McLachlan (1947, p.368).

The integral expressions evaluate to radial Mathieu functions of the first kind, when they are given in one of their several equivalent solutions in terms of

Bessel function series (McLachlan, 1947, §8.30)

$$\mathrm{Ie}_{2n}(\omega;-q) = (-1)^n \frac{\mathrm{ce}_{2n}\left(\frac{\pi}{2};q\right)}{\mathbf{A}_0^{(2n)}} \sum_{r=0}^{\infty} \mathbf{A}_{2r}^{(2n)} \mathrm{I}_{2r}\left[2\sqrt{q}\sinh(\omega)\right] \tag{A-8}$$

$$\mathrm{Ie}_{2n}(\omega;-q) = (-1)^n \frac{\mathrm{ce}_{2n}(0;q)}{\mathbf{A}_0^{(2n)}} \sum_{r=0}^{\infty} (-1)^r \mathbf{A}_{2r}^{(2n)} \mathrm{I}_{2r}\left[2\sqrt{q}\cosh(\omega)\right] \tag{A-9}$$

$$\mathrm{Ie}_{2n+1}(\omega;-q) = (-1)^n \frac{\mathrm{se}'_{2n+1}(0;q)}{\sqrt{q}\mathbf{B}_1^{(2n+1)}} \sum_{r=0}^{\infty} (-1)^r \mathbf{B}_{2r+1}^{(2n+1)} \mathrm{I}_{2r+1}\left[2\sqrt{q}\cosh(\omega)\right] \tag{A-10}$$

$$\mathrm{Io}_{2n+1}(\omega;-q) = (-1)^{n+1} \frac{\mathrm{ce}'_{2n+1}\left(\frac{\pi}{2};q\right)}{\sqrt{q}\mathbf{A}_1^{(2n+1)}} \sum_{r=0}^{\infty} \mathbf{A}_{2r+1}^{(2n+1)} \mathrm{I}_{2r+1}\left[2\sqrt{q}\sinh(\omega)\right] \tag{A-11}$$

Appendix B

Alhargan (2000) has published C++ routines for evaluating Mathieu functions based on the more efficient but less widely applicable continued fraction expansion method. These routines utilize a different normalization scheme than (21) and are only valid for small Mathieu parameter ($q \leq 4n$). We use the more general modern matrix formulation with available matrix solution software (Stamnes and Spjelkavik, 1995; Chaos-Cador and Ley-Koo, 2002), which is valid for any q.

The development of the matrices from which the eigenvalues are computed is found in Green and Michaelson (1965), Delft Numerical Analysis Group (1973), and Stamnes and Spjelkavik (1995). The main and off-diagonals of the infinite matrices, from which the eigenvalues and eigenvectors are computed, are

$$\mathrm{Aev} = \begin{bmatrix} 0 & 4 & 16 & \dots & (2r)^2 & \dots \\ \sqrt{2}q & q & q & \dots & q & \dots \end{bmatrix}, \tag{B-1}$$

$$\mathrm{Aod} = \begin{bmatrix} 1-q & 9 & 25 & \dots & (2r+1)^2 & \dots \\ q & q & q & \dots & q & \dots \end{bmatrix}, \tag{B-2}$$

$$\mathrm{Bod} = \begin{bmatrix} 1+q & 9 & 25 & \dots & (2r+1)^2 & \dots \\ q & q & q & \dots & q & \dots \end{bmatrix}, \tag{B-3}$$

where $\mathbf{A}_{2r}^{(2n)}$ is the matrix of eigenvectors from the symmetric tridiagonal matrix composed of the diagonal (first row) and the off-diagonals (second row) of Aev. Similarly, Aod leads to $\mathbf{A}_{2r+1}^{(2n+1)}$ and Bod leads to $\mathbf{B}_{2r+1}^{(2n+1)}$.

The matrices (B-1–B-3) and the eigenvector matrices derived from them $\mathbf{A}_r^{(n)}, \mathbf{B}_r^{(n)}$ are infinite matrices that must be truncated (at R terms); for the geometries illustrated here $R \leq 20$ is sufficient. Ellipses of very long aspect ratio (large $|q|$) may require larger R (more quantitative relationships for required R are given by Delft Numerical Analysis Group (1973)), but the calculations remain trivial on a desktop computer. For the application considered here, when $A \leq 2$, the expansion of the boundary condition in angular Mathieu functions ($N = 10, R = 16$) is accurate to at least single precision.

Since eigenvectors only define a direction, we normalize them utilizing a convention attributed to Goldstein (1927) and used by McLachlan (1947). It consists of specifying the eigenvectors to be unit length, with special considerations for the zero-order even function. This convention leads to the functions having root mean squared values of $1/\sqrt{2}$ over the interval $0 \leq \psi \leq 2\pi$ (Arscott, 1964, §3).

If LAPACK (or equivalently `eig()` in Matlab) is used to compute the eigenvector matrices, only the first eigenvector of $\mathbf{A}_{2r}^{(2n)}$ must be re-scaled. The solution for $\mathrm{ce}_0(\psi; -q)$ is normalized so it degenerates to $\frac{1}{\sqrt{2}}\cos(0)$ as $q \to 0$. This requires the normalization be

$$2\left[\mathbf{A}_0^{(0)}\right]^2 + \sum_{r=1}^{\infty}\left[\mathbf{A}_r^{(0)}\right]^2 = 1, \tag{B-4}$$

where the first term is included twice.

References

F. A. Alhargan. Algorithm 804: subroutines for the computation of Mathieu functions of integer order. *ACM Transactions on Mathematical Software*, 26(3):408–414, 2000.

F. M. Arscott. *Periodic Differential Equations*. Macmillan, 1964.

F. M. Arscott and A. Darai. Curvilinear co-ordinate systems in which the Helmholtz equation separates. *IMA Journal of Applied Mathematics*, 27: 33–70, 1981.

M. Bakker and J. L. Nieber. Two-dimensional steady unsaturated flow through embedded elliptical layers. *Water Resources Research*, 40:1–12, 2004.

A. Ben-Menahem and S. J. Singh. *Seismic Waves and Sources*. Dover, second edition, 2000.

L. Chaos-Cador and E. Ley-Koo. Mathieu functions revisited: matrix evaluation and generating functions. *Revista Mexicana de Física*, 48(1):67–75, 2002.

L. J. Chu and J. A. Stratton. Elliptical and spheroidal wave functions. *Journal of Mathematics and Physics*, 20(3):259–309, 1941.

412 Delft Numerical Analysis Group. On the computation of Mathieu functions.
413 *Journal of Engineering Mathematics*, 7(1):39–61, 1973.
414 R. J. Duffin. Yukawan potential theory. *Journal of Mathematical Analysis*
415 *and Application*, 35:105–130, 1971.
416 W. R. Gardner. Some steady state solutions of unsaturated moisture flow
417 equations with application to evaporation from a water table. *Soil Science*,
418 85:244–249, 1958.
419 S. Goldstein. Mathieu functions. *Transactions of the Cambridge Philosophical*
420 *Society*, 23(11):303–336, 1927.
421 G. H. Golub and C. F. van Loan. *Matrix Computations*. Johns Hopkins, third
422 edition, 1996.
423 D. J. Green and S. Michaelson. Series solution of certain Sturm-Liouville
424 eigenvalue problems. *The Computer Journal*, 7:322–336, 1965.
425 J. C. Gutiérrez Vega, R. M. Rodriguez Dagnino, A. M. Meneses Nava, and
426 S. Chávez Cerda. Mathieu functions, a visual approach. *American Journal*
427 *of Physics*, 71(3):233–242, 2003.
428 F. Kleinermann, N. J. Avis, and F. A. Alhargan. Analytical solution to the
429 three-dimensional electrical forward problem for an elliptical cylinder. *Phys-*
430 *iological Measurement*, 23:141–147, 2002.
431 A. Klute. A numerical method for solving the flow equation for water in
432 unsaturated materials. *Soil Science*, 73:105–116, 1952.
433 F. Kucûk and W. E. Brigham. Transient flow in elliptical systems. *Society of*
434 *Petroleum Engineers Journal*, 267:401–410, 1979.
435 D. O. Lomen and A. W. Warrick. Linearized moisture flow with loss at the
436 soil surface. *Soil Science Society of America Journal*, 42:396–400, 1978.
437 R. Maertens and R. Rousseau. A new formula approach for the circumference
438 of an ellipse. *Wiskunde & Onderwijs*, 26:249–258, 2000.
439 MathWorks. *MATLAB*, 7.5 edition, 2007.
440 N. W. McLachlan. *Theory and Application of Mathieu Functions*. Oxford,
441 1947.
442 P. Moon and D. E. Spencer. *Field Theory for Engineers*. D. Van Nostrand,
443 1961a.
444 P. Moon and D. E. Spencer. *Field Theory Handbook: Including coordinate*
445 *systems differential equations and their solutions*. Springer-Verlag, 1961b.
446 P. M. Morse and H. Feshbach. *Methods of Theoretical Physics*, volume 1 and
447 2. McGraw-Hill, 1953.
448 S. A. Orszag. *Science and Computers*, volume 10 of *Advances in Mathematics*
449 *Supplementary Studies*, chapter Fast Eigenfunction Transforms. Academic
450 Press, 1986.
451 J. R. Philip. Steady infiltration from buried point sources and spherical cavi-
452 ties. *Water Resources Research*, 4(5):1039–1047, 1968.
453 J. R. Philip. Steady infiltration from circular cylindrical cavities. *Soil Science*
454 *Society of America Journal*, 48:270–278, 1984.
455 J. R. Philip. Multidimensional steady infiltration to a water table. *Water*

Resources Research, 25(1):109–116, 1989.

A. J. Pullan. The quasilinear approximation for unsaturated porous media flow. *Water Resources Research*, 26(6):1219–1234, 1990.

W. J. Rawls, D. L. Brakensiek, W. J. Elliot, and J. M. Laflen. Prediction of furrow irrigation final infiltration rate. *Transactions of the American Society of Agricultural Engineers*, 33(5):1601–1604, 1990.

L. A. Richards. Capillary conduction of liquid through porous mediums. *Physics*, 1:318–333, 1931.

T. H. Skaggs, T. J. Trout, J. Šimunek, and P. J. Shouse. Comparison of HYDRUS-2D simulations of drip irrigation with experimental observations. *Journal of Irrigation and Drainage Engineering*, 130(4):304–310, 2004.

J. J. Stamnes and B. Spjelkavik. New method for computing eigenfunctions (Mathieu functions) for scattering by elliptical cylinders. *Pure and Applied Optics*, 4(3):251–262, 1995.

J. A. Stratton. *Electromagnetic Theory*. McGraw-Hill, 1941.

C. J. Tranter. Heat conduction in the region bounded internally by an elliptical cylinder and an analogous problem in atmospheric diffusion. *Quarterly Journal of Mechanics and Applied Mathematics*, 4(4):461–465, 1951.

A. W. Warrick. *Soil Water Dynamics*. Oxford, 2003.

A. W. Warrick and N. Lazarovitch. Infiltration from a strip source. *Water Resources Research*, 43:W03420, 2007.

A. W. Warrick, N. Lazarovitch, A. Furman, and D. Zerihun. Explicit infiltration for furrows. *Journal of Irrigation and Drainage Engineering*, 133(4): 307–313, 2007.

G. N. Watson. *A Treatise on the Theory of Bessel Functions*. Cambridge, second edition, 1944.

R. A. Wooding. Steady infiltration from a shallow circular pond. *Water Resources Research*, 4(6):1259–1273, 1968.

	circular	horizontal ellipse			vertical ellipse		
e	0	1	0.9	0.5	1	0.9	0.5
c_0	1.7054	1.2021	1.3975	1.6344	1.0991	1.3364	1.6199
c_1	2.3638	2.1901	2.2727	2.3411	2.1291	2.3231	2.3636
c_2	-0.2747	-0.8789	-0.5527	-0.3298	-0.7294	-0.3172	-0.2678
c_3	-0.1700	-0.4488	-0.2977	-0.1951	-0.3603	-0.1813	-0.1651

Table 1
Rational polynomial regression coefficients for $Q(A)$ in (53)

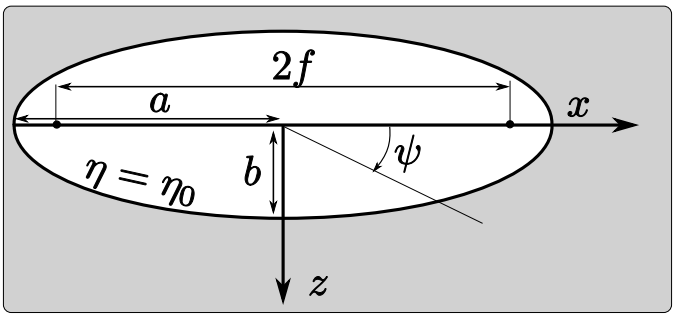

Fig. 1. Elliptical coordinates η (radial) and ψ (angular); a, b, and f are the semi–major, -minor, and -focal lengths.

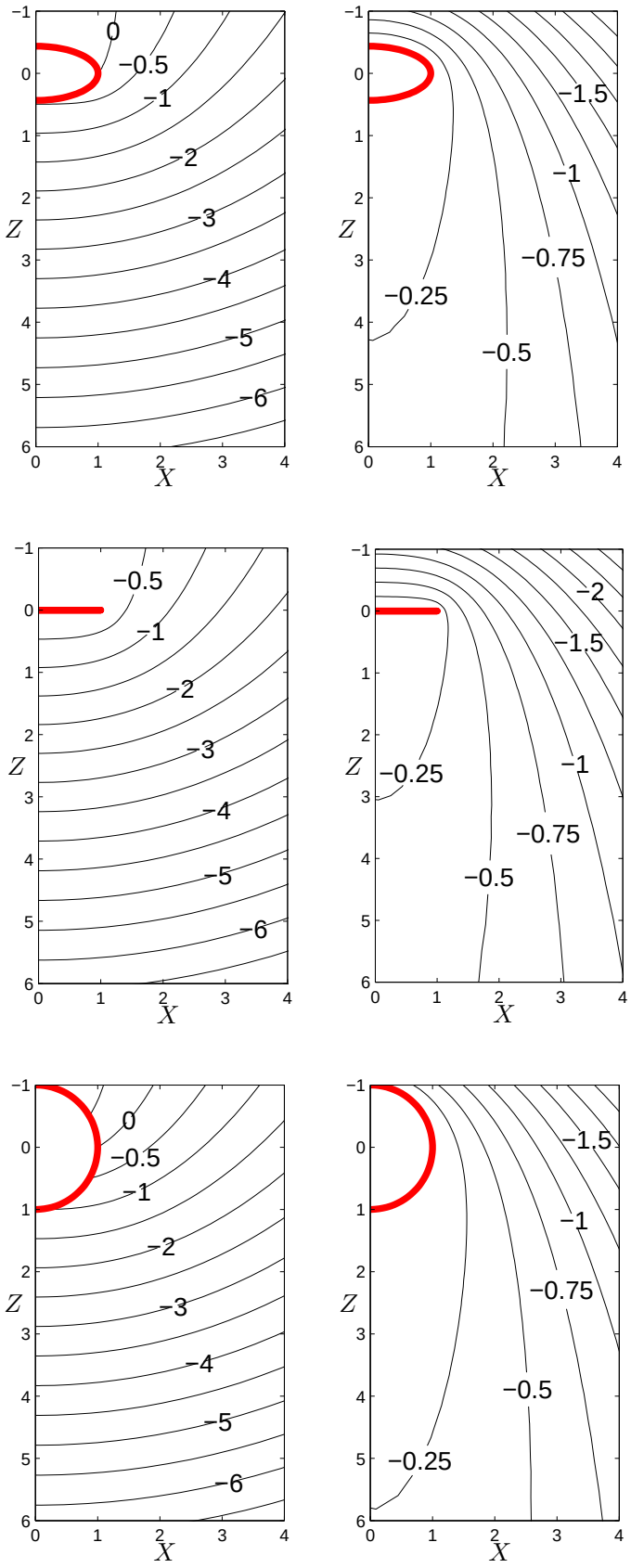

Fig. 2. Contours of dimensionless hydraulic head, $\mathbf{\Phi}$, (left) and pressure head, $\mathbf{\Psi}$, (right) for horizontal ellipses ($A = 1.0$, ~~ℓ~~ $= [0.9, 1.0, 0.01]$)

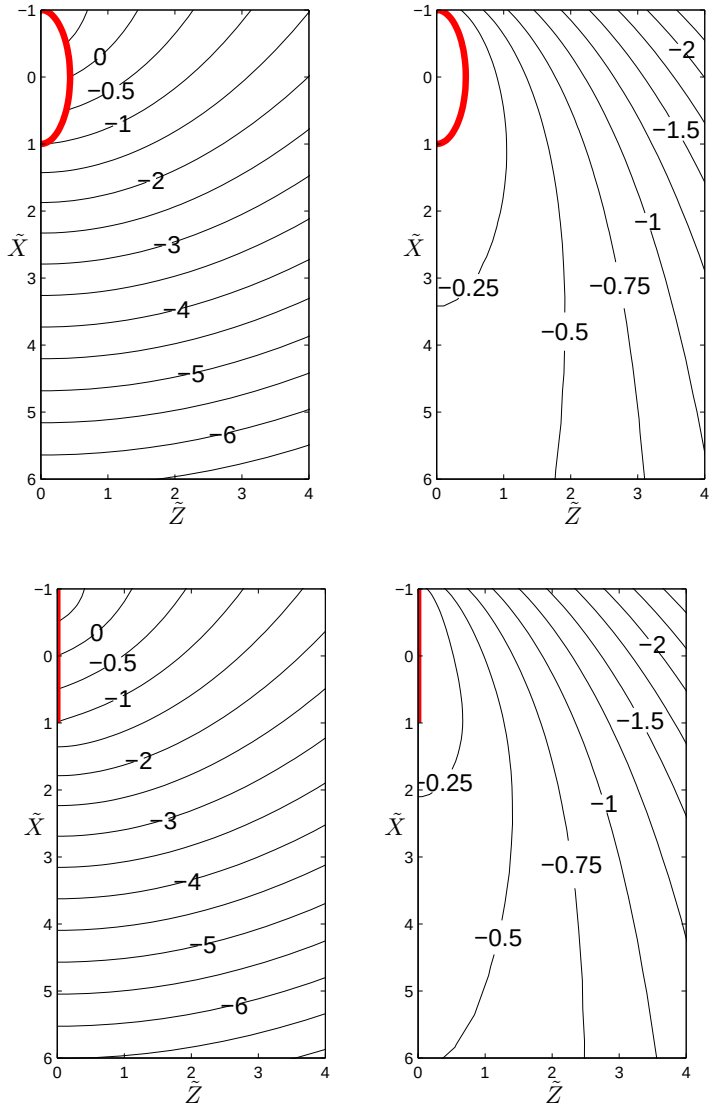

Fig. 3. Contours of dimensionless hydraulic head, $\tilde{\mathbf{\Phi}}$, (left) and pressure head, $\tilde{\mathbf{\Psi}}$, (right) for vertical ellipse ($A = 1.0$, $e = [0.9, 1.0]$)

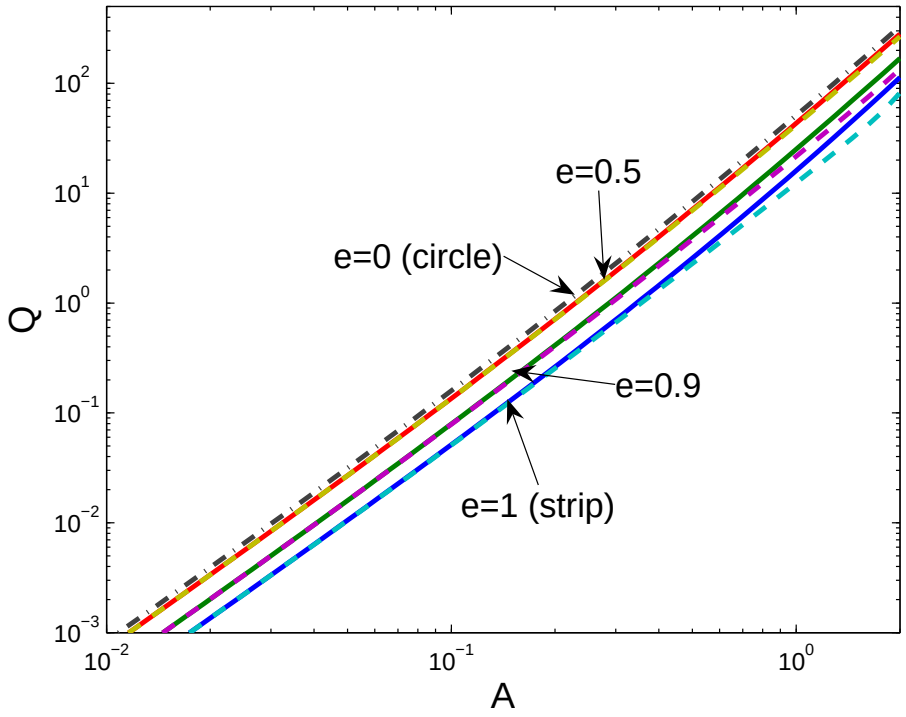

Fig. 4. Log-log plot of dimensionless flowrate, $Q = C\overline{V}_0$, as a function of size (A) and shape (e) of the horizontal (solid lines) and vertical (dashed lines) cavities. Limiting circular case is upper dash-dot line.

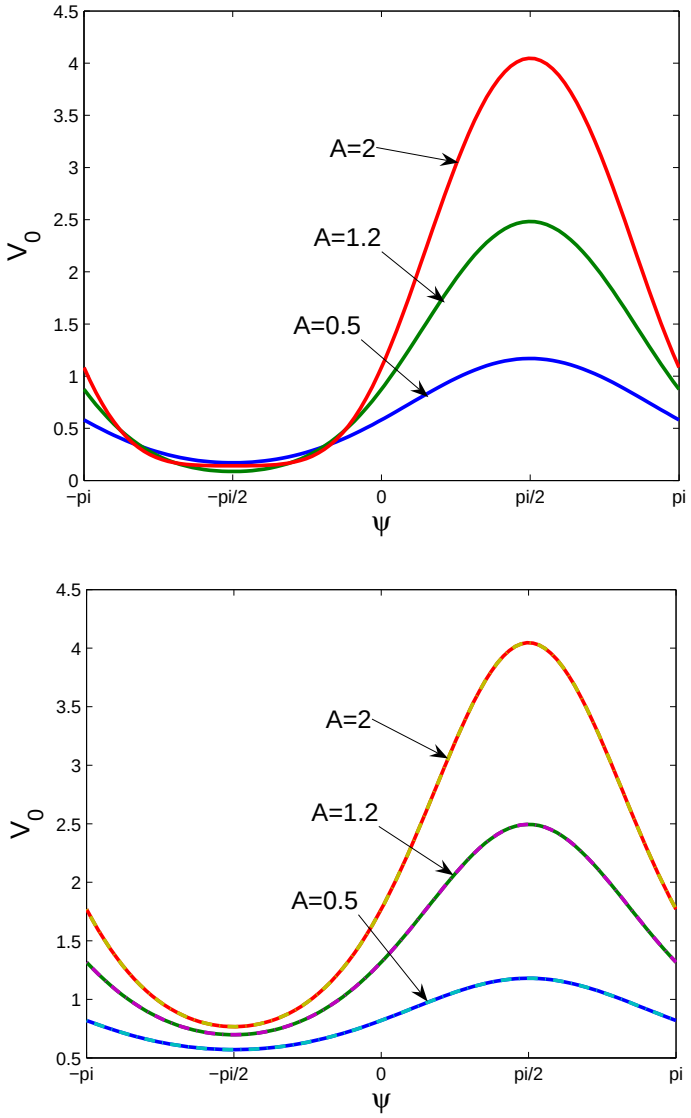

Fig. 5. Distribution of dimensionless normal flux, V_0, with angle, ψ, for horizontal strip (left, $e = 1$) and horizontal near-circular (right, $e = 0.01$) cases (true circular solution shown as nearly coincident dash-dot line)